Received 26 July 2020; revised 19 August 2020; accepted 29 August 2020. Date of publication 1 September 2020; date of current version 22 September 2020.
The review of this article was arranged by Editor S. Menzel.

Digital Object Identifier 10.1109/JEDS.2020.3020893

Impact of Surface Treatments and Post-Deposition Annealing Upon Interfacial Property of ALD-Al_2O_3 on a-Plane GaN

YANNI ZHANG, JINCHENG ZHANG (Member, IEEE), ZHUANGZHUANG HU, ZHAOQING FENG, HEPENG ZHANG, SHENGRUI XU, ZHIHONG LIU (Senior Member, IEEE), HONG ZHOU (Member, IEEE), AND YUE HAO (Senior Member, IEEE)

Laboratory of Wide BandGap Semiconductor Materials and Devices, School of Microelectronics, Xidian University, Xi'an 710071, China

CORRESPONDING AUTHORS: J. ZHANG and H. ZHOU (e-mail: jchzhang@xidian.edu.cn; hongzhou@xidian.edu.cn)

This work was supported in part by the National Key Research and Development Program under Grant 2016YFB0400100, in part by the Project under Grant JZX7X20191183000201, in part by the National Key Science and Technology Special Project under Grant 2017ZX01001301, and in part by Wuhu and Xidian University special fund for industry-university-research cooperation under Grant XWYCXY-012019002.

ABSTRACT Optimization of interface characteristics between dielectric and non-polar GaN surface is very important and urgent for vertical GaN MOS device whose channel is perpendicular to the conventional c-plane. In this work, the effects of piranha cleaning and N_2 post deposition annealing (PDA) to the interface between atomic-layer-deposited (ALD)-Al_2O_3 and a-plane GaN samples were comprehensively investigated by X-ray photoelectron spectroscopy (XPS), atomic force microscopy (AFM) and photo-assisted capacitance-voltage (C-V) measurements. The piranha cleaning and N_2 annealing can improve interface characteristics through the reduction in surface roughness and Ga-O bonds, respectively. Therefore, the frequency dispersion and hysteresis are nearly suppressed with a low interface trap quantity (Q_{it}) of 4.1×10^{11} cm^{-2} and a low average interface state density (D_{it}) of 2.04×10^{11} $cm^{-2} \cdot eV^{-1}$ from photo-assisted C-V measurements, showing the great promise of utilizing piranha pretreatment, buffered oxide etch (BOE) dip, and N_2 annealing as an effective route to improve the vertical GaN MOS interface properties.

INDEX TERMS GaN, a-plane, Interface trap density, ALD-Al_2O_3, photo-assisted C-V measurement.

I. INTRODUCTION

Due to its wide bandgap, high electron mobility and saturation velocity [1], [2] gallium nitride (GaN) turns out to be a competitive candidate for both power switch and power amplifier applications [3]–[9]. In recent 20 years, both industry and academia have witnessed the significant progress of GaN high-electron-mobility transistors (HEMTs), mainly because of the polarization induced high density, high mobility and high velocity electrons at the c-plane [10]. On the other hand, vertical GaN power device is attracting more attention due to the maturity of the GaN native substrate and the demonstration of various state-of-art high performance power devices [11]–[13]. In particular, vertical metal-oxide-semiconductor field-effect transistors (MOSFETs) with the capability of delivering higher blocking voltage and on-current have shown their great promise to extend the application voltage beyond the general acquiesced 600 V from p-GaN gate-injection-transistors (GITs) [14], [15]. In general, this vertical non-polar a-plane or m-plane channel is perpendicular to the c-plane so that the interface between non-polar GaN and gate dielectric should be carefully investigated to gain a better understanding about the interfacial properties.

There are several studies about the band offset characterizations of atomic layer deposition (ALD) Al_2O_3 on m-plane GaN by X-ray photoelectron spectroscopy (XPS) and the interface property investigations of Al_2O_3, SiO_2 and high-k dielectrics on non-polar GaN [16]–[18]. However, it seems there are still some frequency dispersion and hysteresis observed and there is no in-depth study on the effects

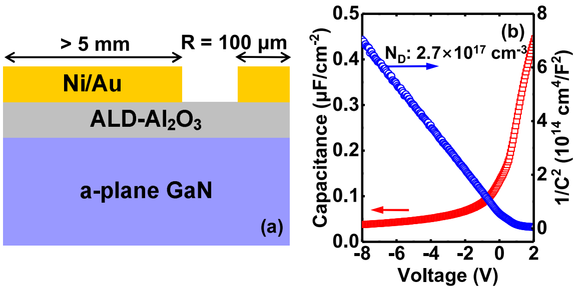

FIGURE 1. (a) Schematic cross-section of fabricated Al_2O_3/a-plane GaN MOSCAP. (b) C-V and $1/C^2$-V characteristics of the Al_2O_3/a-plane GaN MOSCAP with extract electron concentration of 2.7×10^{17} cm^{-3}.

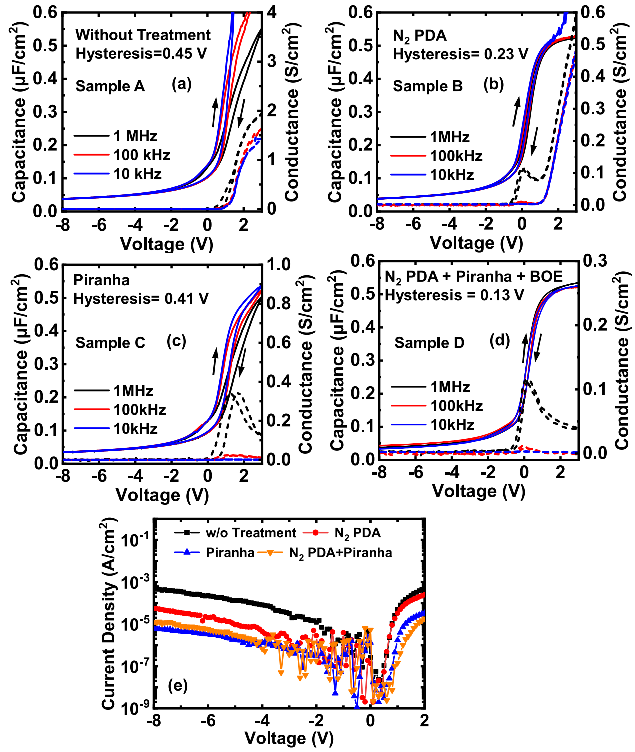

FIGURE 2. (a) - (d) C-V (solid line) and G-V curves (dashed line) of Al_2O_3/a-plane GaN MOSCAPs with different treatments measured at 10 kHz, 100 kHz and 1 MHz. The sweep rate for the C-V hysteresis measurement is 0.1 second per 0.01 V step. (e) Current density-voltage (J-V) characteristics of a-plane GaN MOSCAPs.

of surface treatment and post-deposition annealing process upon non-polar GaN and dielectrics interfaces, which is the key to reduce the interface state and obtain excellent vertical MOSFET characteristics.

In this work, we report on implementing various surface treatments and post-deposition annealing methodologies to improve the interface quality between the ALD-Al_2O_3 and a-plane non-polar GaN. In addition, various characterization techniques by XPS, atomic force microscopy (AFM), conductance method and photo-assisted C-V measurements are incorporated to provide guidance for improving the performances of GaN MOS devices.

II. EXPERIMENTAL PROCEDURE

The four a-plane Si-doped GaN samples were sliced from c-plane GaN, which is grown by hybrid vapor phase epitaxy (HVPE). The samples preparation started with ultrasonic cleaning in acetone and ethanol for 10 minutes and DI water rinse. 15 nm Al_2O_3 was deposited on all samples by ALD at 300°C with tri-methylaluminum (TMA) and ozone (O_3) as oxygen source. Five different treatments were adopted on those samples: (A) without treatment; (B) only 5 mins N_2 annealing at 500°C after Al_2O_3 deposition; (C) only 1 min piranha (H_2O_2:H_2SO_4 = 3:7) cleaning before Al_2O_3 deposition; (D) 1 min piranha cleaning and 30s BOE (49% HF:40% NH_4F = 1:6) dipped before Al_2O_3 deposition and followed the ALD Al_2O_3 growth, 5 mins of N_2 annealing at 500°C was further used. Series MOS capacitors (MOSCAPs) were then defined by photo-lithography, depositing Ni/Au (60/120 nm) metal stacks and lift-off processes. The cross-section schematic view of MOSCAP for measurements is shown in Fig. 1(a) which is obtained by connecting one large and one small capacitor in series (the large capacitor can be ignored). The Keithley 4200A-SCS parameter analyzer with heated chuck was used for all the C-V measurements. A deep UV light with wavelength of 365 nm was used as the light source during the photo-assisted C-V measurements.

III. RESULTS AND DISCUSSION

Fig. 1(b) shows the doping concentration of the a-plane GaN, and it is determined to be 2.7×10^{17} cm^{-3} from the $d(1/C^2)/dV$ [19] of the C-V measurements at 100 kHz. Fig. 2 shows the f-dependent C-V and G-V hysteresis loop of the Al_2O_3/a-plane GaN MOSCAPs, which were measured at room temperature (RT) and the hysteresis was calculated at 1 MHz. The f-dependent C-V measurements start from biasing the diode from depletion to accumulation with 0.01 V as a step and then sweeping back to depletion. Traps located at the interface of the oxide and bulk semiconductor may trap and de-trap electrons at this bi-directional sweeps. This feature leads to a shift of the flat-band voltage (V_{FB}) during the C-V measurement. The hysteresis is determined by its maximum value at 1 MHz. Sample A without any treatment demonstrates large dispersion, hysteresis, and high interface trap quantity (Q_{it}). The significant increase in capacitance at lower frequencies is caused by larger leakage as shown in Fig. 2(e). And samples without piranha clean show large conductance at forward bias which also indicates the leakage over the MOSCAPs. The hysteresis of sample B with N_2 PDA is 0.23 V and small dispersion is also obtained in sample B. Sample C shows large hysteresis of 0.41 V but low leakage. The treatment combined N_2 PDA and piranha cleaning in sample D obtains the smallest hysteresis of 0.13 V, low frequency dispersion and unobservable leakage.

The detectable Q_{it} can be roughly estimated by using the equation: $Q_{it} = C_{ox} \times \Delta V/q$, where C_{ox} is calculated oxide capacitance of 0.5 μF/cm² and ΔV is V_{FB} shift,

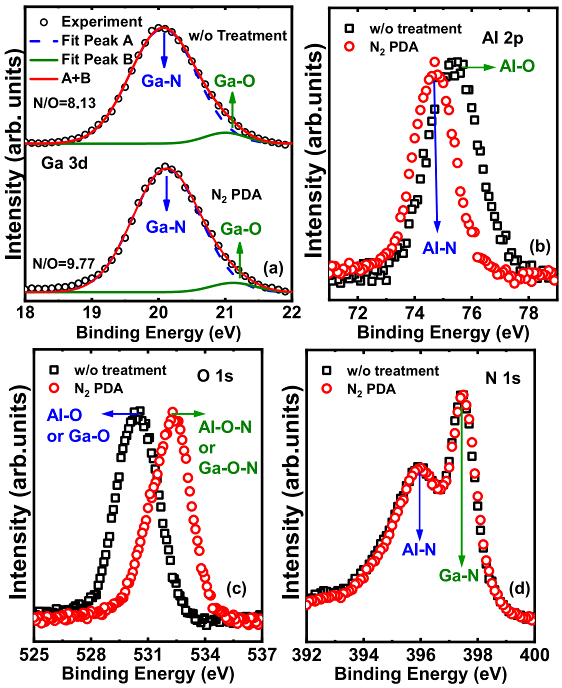

FIGURE 3. XPS spectra of (a) Ga 3d, (b) Al 2p, (c) O 1s, and (d) N 1s core-level of 2 nm ALD Al_2O_3 on a-plane GaN with or without N_2 PDA, respectively. All binding energies have been charge referenced to the primary carbon C-C peak at 284.8 eV.

respectively [20]. The Q_{it} can be reduced from 1.4×10^{12} cm^{-2} to 7.3×10^{11} cm^{-2} by N_2 PDA. As shown in Fig. 3, the bonding states in ALD Al_2O_3 on a-plane GaN with or without N_2 PDA were also studied with XPS. The ratio of Ga-N bond to Ga-O bond at interface increases from 8.13 to 9.77 by 5 mins of N_2 PDA at 500°C. The improvement in Q_{it} may be due to the reduction of Ga-O bond after N_2 PDA. The higher oxidation states of Ga reflected in Ga-O bond have been considered as one of the factors that introduce a high interfacial defect density and traps [21], [22]. The Al 2p peak position shifted from 75.5 eV to 74.7 eV after N_2 PDA which suggests the increase of Al-N bonds during N_2 PDA [23]. The O 1s peak position shifted from 530.28 eV to 532.3 eV after N2 PDA also suggests the transition from Al-O (or Ga-O) bonds to Al-O-N (or Al-O-N) bonds [21], [24]. The XPS spectra of N 1s core levels is basically not affected by N_2 PDA which may be due to the simultaneous increase of the bonds related to Ga-N and Al-N. The minimal $Q_{it} = 4.1 \times 10^{11}$ cm^{-2} of sample D may be attributed to 30 s BOE dipped after piranha cleaning which reduces residual oxides during the piranha treatment process. According to XPS data shown in Fig. 4(a), C-O (the peak around 286 eV may also be the C-N bonds) [25] and C = O [26] bonds are effectively reduced by piranha and BOE cleaning. The root mean square (RMS) surface roughness of a-plane GaN were measured by AFM and shown in Fig. 4(b). The results indicated that piranha cleaning can effectively improve surface RMS from 0.405 to 0.180 nm which contributes to the minimized leakage path [27].

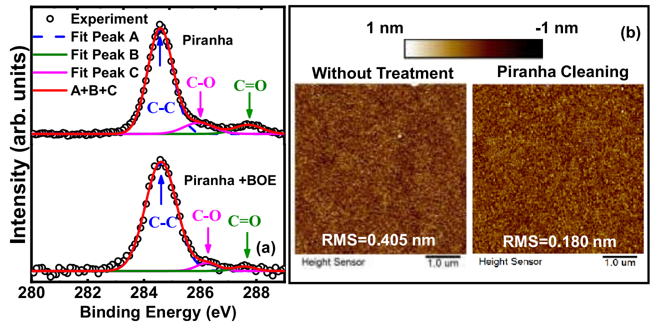

FIGURE 4. (a) XPS C 1s core levels of a-plane GaN samples with piranha cleaning and with both piranha and BOE cleaning, respectively. All binding energies have been charge referenced to the primary carbon C-C peak at 284.8 eV. (b) Atomic force microscopy images of a-plane GaN pretreated with or without piranha cleaning, respectively.

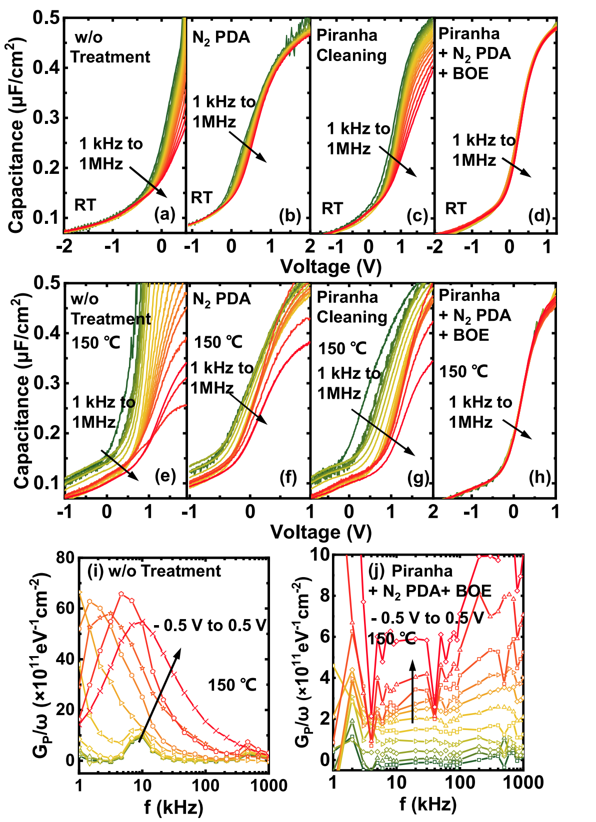

FIGURE 5. F-dependent C-V measurements of different MOSCAPs at RT or 150°C: (a) and (e) without treatment, (b) and (f) N_2 PDA, (c) and (g) piranha cleaning, and (d) and (h) both piranha cleaning and N_2 PDA. Extracted $G_p/Aq\omega$ of (i) sample A and (j) sample D at T = 150°C from AC conductance method. The step of the C-V-f measurement is 0.1 V.

Due to the wide bandgap nature of the GaN, the RT C-V characterization is not sufficient to detect the trap states [28], [29], which locates away from the conduction band (E_C) minimal. In order to detect deeper trap states in the bandgap, a high-T C-V measurement is desirable. The C-V curves from 1 kHz to 1 MHz at RT and 150°C are presented in Fig. 5 (a) to (h). Sample A, sample B and sample C exhibit a large dispersion phenomenon, and C-V characteristics are severely degraded at 150°C. Combining the N_2 PDA, piranha cleaning, and BOE dipped, the excellent interface characteristic has been obtained as shown in Fig. 5(d) and (h). The conventional conductance method was first thought to be able to accurately measure interface traps density (D_{it}). The parallel conductance (G_p/ω) can be calculated from the measured capacitance (C_m) and conductance (G_m) by using the equation: $G_p/\omega = \omega C_{OX}^2 Gm/[G_m^2 + \omega^2(C_{ox} - C_m)]$ [19], where ω is radial frequency. And the energy level of traps (E_T) with respect to GaN conduction band minimum (E_C) of the interface states can be found by the SRH (Shockley-Read-Hall) model using the equation: $(E_C - E_T) = k_B T \ln(\tau_{it} \sigma \nu_t N_C)$ [19], where k_B is the Boltzmann constant, T is the temperature, τ_{it} is the lifetime of the interface states, σ is the capture cross section of the interface states, ν_t is the thermal velocity, and N_C is effective density of state in the conduction band. Although the conductance ($G_p/Aq\omega$) peaks of sample A can be obtained by the conventional conductance method at 150 °C as shown in Fig. 4(i), but no obvious normalized conductance ($G_p/Aq\omega$) peak is observable (shown in Fig. 5 (j)) even at T = 150 °C for sample D. It is a common phenomenon of wide bandgap materials with undetectable trap level due to the large bandgap in semiconductor and deep level of traps [30]–[32].

On the other hand, with the assistance of the ultraviolet (UV) illumination to generate hole and electron pairs, the photo-assisted C-V method can make sure that the traps at different energies in the bandgap can respond to the measurement signal during the C-V measurement, making it possible to evaluate the quality and calculate average D_{it} of our fabricated MOSCAPs. In order to avoid traps not being completely filled with electrons, the measurements started with biasing gate voltage at accumulation for 10 s. And then C-V measurements from deep depletion to accumulation at f = 1 MHz in dark to achieve dark C-V curve in Fig. 6. The automatic switching test program function of Keithley 4200A-SCS parameter analyzer is used to conduct continuous testing. Next, the gate bias is kept at −10 V, while holding UV light illumination for 10 minutes to force the generated holes toward the Al_2O_3/GaN interface. The large hole concentration at the interface under illumination enables the interface states to change from allowing electrons to occupy to recombine. After that, turning off the UV light and then the same C-V measurements were performed again to acquire a post-UV C-V curve. The holes generated by UV illumination recombined with those electrons captured in traps make Al_2O_3/GaN interface donor-like. Compared to acceptor-like interface before UV illumination, a shift of the C-V curves can be observed. This shift can be quantitatively described by ΔV_F, while the averaged D_{it} can be obtained by the following equation [33]:

$$D_{it} = \frac{C_{ox} \times \Delta V_F}{q \times E_g} \tag{1}$$

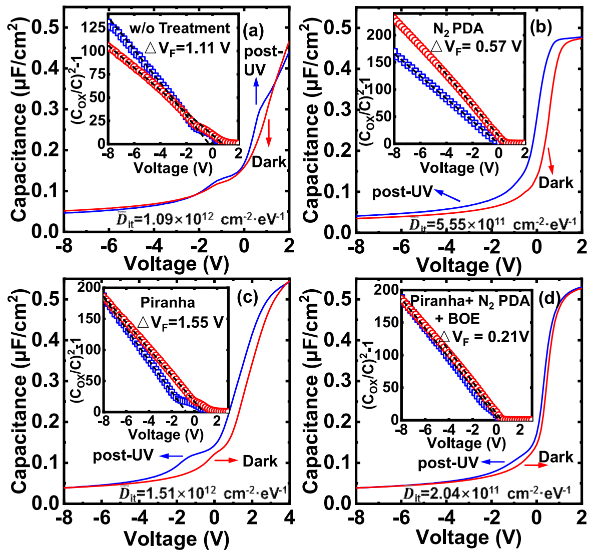

FIGURE 6. Photo-assisted C-V measurements of MOSCAPs with different treatments: (a) without treatment, (b) N_2 PDA, (c) piranha cleaning and (d) piranha cleaning and N_2 PDA. The insets illustrate the $(C_{ox}/C)^2$-1 as a function of voltage to extract the ΔV of each sample. The sweep rate for the C-V measurement is 0.1 second per 0.01 V step.

The ΔV_F is the shift of V_{FB}. And V_{FB} is determined through the extrapolated line of the $(C_{ox}/C)^2 - 1 \sim V_G$ at $(C_{ox}/C)^2 - 1 = 0$ [34]. The C-V curves both in dark and after UV irradiated for different treatments have been shown in Fig. 5, and the insets show the V_{FB} shift. The ideal V_{FB} of 15 nm Al_2O_3 on a-plane GaN is 1.1 V simulated by TCAD. The negatively shifting in V_{FB} for the capacitors with N_2 PDA is due to the decreasing negative effective oxide charge at the Al_2O_3/GaN interface [35]. The piranha and BOE cleaning before Al_2O_3 deposition and N_2 PDA can significantly reduce the ΔV_F from 1.11 V in sample A to 0.21 V and achieve minimal averaged interface trap state density to 2.04×10^{11} cm^{-2}·eV^{-1}.

IV. CONCLUSION

The interfaces of ALD-Al_2O_3 on a-plane GaN by various treatments were characterized by XPS, AFM and photo-assisted C-V measurements. The N_2 PDA reduces C-V hysteresis through the reduction of Ga-O bonds, and piranha cleaning suppressed leakage by improvement of surface RMS. Combining piranha and BOE cleaning before Al_2O_3 deposition and N_2 PDA, a low average D_{it} of 2.04×10^{11} cm^{-2}·eV^{-1} by photo-assisted C-V measurements were achieved, demonstrating its great potential as an effective approach to improve the vertical GaN MOS interface properties.

REFERENCES

[1] S. Joblot, F. Semond, Y. Cordier, P. Lorenzini, and J. Massies, “High-electron-mobility AlGaN/GaN heterostructures grown on Si(001) by molecular-beam epitaxy,” *Appl. Phys. Lett.*, vol. 87, no. 13, Sep. 2005, Art. no. 133505, doi: 10.1063/1.2067698.

[2] L. Ardaravičius *et al.*, "Electron drift velocity in AlGaN/GaN channel at high electric fields," *Appl. Phys. Lett.*, vol. 83, no. 19, p. 4038, Nov. 2003, doi: 10.1063/1.1626258.

[3] F. A. Ponce and D. P. Bour, "Nitride-based semiconductors for blue and green light-emitting devices," *Nature*, vol. 386, pp. 351–359, Mar. 1997, doi: 10.1038/386351a0.

[4] O. B. Shchekin *et al.*, "High performance thin-film flip-chip InGaN-GaN light-emitting diodes," *Appl. Phys. Lett.*, vol. 89, no. 7, Aug. 2006, Art. no. 071109, doi: 10.1063/1.2337007.

[5] F. Medjdoub *et al.*, "Low on-resistance high-breakdown normally off AlN/GaN/AlGaN DHFET on Si substrate," *IEEE Electron Device Lett.*, vol. 31, no. 2, pp. 111–113, Feb. 2010, doi: 10.1109/LED.2009.2037719.

[6] H. Zhou *et al.*, "High-performance InAlN/GaN MOSHEMTs enabled by atomic layer epitaxy MgCaO as gate dielectric," *IEEE Electron Device Lett.*, vol. 37, no. 5, pp. 556–559, May 2016, doi: 10.1109/LED.2016.2537198.

[7] H. Ohta *et al.*, "Vertical GaN p-n junction diodes with high breakdown voltages over 4 kV," *IEEE Electron Device Lett.*, vol. 36, no. 11, pp. 1180–1182, Nov. 2015, doi: 10.1109/LED.2015.2478907.

[8] Y. Yue *et al.*, "InAlN/AlN/GaN HEMTs with regrown ohmic contacts and f_T of 370 GHz," *IEEE Electron Device Lett.*, vol. 33, no. 7, pp. 988–990, Jul. 2012, doi: 10.1109/LED.2012.2196751.

[9] Y. Tang *et al.*, "Ultra-high-speed GaN high-electron-mobility transistors with f_T/f_{max} of 454/444 GHz," *IEEE Electron Device Lett.*, vol. 36, no. 6, pp. 549–551, Jun. 2015, doi: 10.1109/LED.2015.2421311.

[10] B. S. Eller, J. Yang, and R. J. Nemanich, "Polarization effects of GaN and AlGaN: Polarization bound charge, band bending, and electronic surface states," *J. Electron. Mater.*, vol. 43, no. 6, pp. 4560–4568, Sep. 2014, doi: 10.1007/s11664-014-3383-z.

[11] W. Li and S. Chowdhury, "Design and fabrication of a 1.2 kV GaN-based MOS vertical transistor for single chip normally off operation," *Phys. Status Solidi*, vol. 213, no. 10, pp. 2714–2720, Jun. 2016, doi: 10.1002/pssa.201532575.

[12] C. Gupta *et al.*, "In situ oxide, GaN interlayer-based vertical trench MOSFET (OG-FET) on bulk GaN substrates," *IEEE Electron Device Lett.*, vol. 38, no. 3, pp. 353–355, Mar. 2017, doi: 10.1109/LED.2017.2649599.

[13] T. Oka, Y. Ueno, T. Ina, and K. Hasegawa, "Vertical GaN-based trench metal oxide semiconductor field-effect transistors on a free-standing GaN substrate with blocking voltage of 1.6 kV," *Appl. Phys. Exp.*, vol. 7, no. 2, Jan. 2014, Art. no. 021002, doi: 10.7567/APEX.7.021002.

[14] Y. Uemoto *et al.*, "Gate injection transistor (GIT)—A normally-off AlGaN/GaN power transistor using conductivity modulation," *IEEE Trans. Electron Devices*, vol. 54, no. 12, pp. 3393–3399, Dec. 2007, doi: 10.1109/TED.2007.908601.

[15] T. Katsuno, M. Kanechika, K. Itoh, K. Nishikawa, T. Uesugi, and T. Kachi, "Improvement of current collapse by surface treatment and passivation layer in p-GaN Gate GaN high-electron-mobility transistors," *Jpn. J. Appl. Phys.*, vol. 52, p. 04CF08, Apr. 2013, doi: 10.7567/JJAP.52.04CF08.

[16] X. Wu *et al.*, "Improved interface properties of GaN metal-oxide-semiconductor device with non-polar plane and AlN passivation layer," *Appl. Phys. Lett.*, vol. 109, no. 23, Dec. 2016, Art. no. 232101, doi: 10.1063/1.4971352.

[17] Y. Jia, J. Wallace, and J. Gardella, "Interface characterization of atomic layer deposited Al_2O_3 on m-plane GaN," *Phys. Status Solidi B*, vol. 254, no. 8, Aug. 2017, Art. no. 1600681, doi: 10.1002/pssb.201600681.

[18] Y. Jia, K. Zeng, and U. Singisetti, "Interface characterization of atomic layer deposited high-k on non-polar GaN," *J. Appl. Phys.*, vol. 122, no. 15, Oct. 2017, Art. no. 154104, doi: 10.1063/1.4986215.

[19] D. K. Schroder, *Semiconductor Material and Device Characterization*, 3rd ed. Hoboken, NJ, USA: Wiley, 2006, doi: 10.1063/1.2810086.

[20] H. Zhou, S. Alghamdi, M. Si, G. Qiu, and P. D. Ye, "Al_2O_3/β-Ga_2O_3 (-201) interface improvement through piranha pretreatment and postdeposition annealing," *IEEE Electron Device Lett.*, vol. 37, no. 11, pp. 1411–1414, Nov. 2016, doi: 10.1109/LED.2016.2609202.

[21] C. R. English *et al.*, "Impact of surface treatments on high-κ dielectric integration with Ga-polar and N-polar GaN," *J. Vac. Sci. Technol., B*, vol. 32, no. 3, 2014, Art. no. 03D106, doi: 10.1116/1.4831875.

[22] S. Yang *et al.*, "High-quality interface in Al_2O_3/GaN/AlGaN/GaN MIS structures with in situ pre-gate plasma nitridation," *IEEE Electron Device Lett.*, vol. 34, no. 12, pp. 1497–1499, Dec. 2013, doi: 10.1109/LED.2013.2286090.

[23] L. Rosenberger, B. Ronald, M. Erik, A. Gregory, and S. Gina, "XPS analysis of aluminum nitride films deposited by plasma source molecular beam epitaxy," *Surf. Interface Anal.*, vol. 40, no. 9, pp. 1254–1261, 2008, doi: 10.1002/sia.2874.

[24] Z. Feng *et al.*, "Band alignment of $SiO_2/(Al_xGa_{1-x})_2O_3$ ($0 \leq x \leq 0.49$) determined by X-ray photoelectron spectroscopy," *Appl. Surf. Sci.*, vol. 434, pp. 440–444, 2018, doi: 10.1016/j.apsusc.2017.10.156.

[25] M. Rusop, T. Soga, and T. Jimbo, "X-ray photoelectron spectroscopy studies on the bonding properties of oxygenated amorphous carbon nitride thin films synthesized by pulsed laser deposition at different substrate temperatures," *J. Non-Cryst. Solids*, vol. 351, nos. 49–51, pp. 3738–3746, Dec. 2005, doi: 10.1016/j.jnoncrysol.2005.09.020.

[26] U. Gelius *et al.*, "Molecular spectroscopy by means of ESCA III. Carbon compounds," *Physica Scripta*, vol. 2, nos. 1–2, pp. 70–80, 1970, doi: 10.1088/0031-8949/2/1-2/014.

[27] T. Hossain *et al.*, "Effect of GaN surface treatment on Al_2O_3/n-GaN MOS capacitors," *J. Vac. Sci. Technol. B*, vol. 33, no. 6, Sep. 2015, Art. no. 061201, doi: 10.1116/1.4931793.

[28] M. Miczek, C. Mizue, T. Hashizume, and B. Adamowicz, "Effects of interface states and temperature on the *C-V* behavior of metal/insulator/AlGaN/GaN heterostructure capacitors," *J. Appl. Phys.*, vol. 103, no. 10, May 2008, Art. no. 104510, doi: 10.1063/1.2924334.

[29] S. Yang *et al.*, "Mapping of interface traps in high-performance Al_2O_3/AlGaN/GaN MIS-heterostructures using frequency- and temperature-dependent C-V techniques," in *Proc. IEEE Int. Electron Devices Meeting*, Washington, DC, USA, 2013, pp. 1–4, doi: 10.1109/IEDM.2013.6724573.

[30] R. Yeluri, B. L. Swenson, and U. K. Mishra, "Interface states at the SiN/AlGaN interface on GaN heterojunctions for Ga and N-polar material," *J. Appl. Phys.*, vol. 111, no. 4, Feb. 2012, Art. no. 043718, doi: 10.1063/1.3687355.

[31] Y. Q. Wu, T. Shen, P. D. Ye, and G. D. Wilk, "Photo-assisted capacitance-voltage characterization of high-quality atomic-layer-deposited Al_2O_3/GaN metal-oxide-semiconductor structures," *Appl. Phys. Lett.*, vol. 90, no. 14, Apr. 2007, Art. no. 143504, doi: 10.1063/1.2719228.

[32] B. L. Swenson and U. K. Mishra, "Photoassisted high-frequency capacitance-voltage characterization of the Si_3N_4/GaN interface," *J. Appl. Phys.*, vol. 106, no. 6, Sep. 2009, Art. no. 064902, doi: 10.1063/1.3224852.

[33] J. Tan, M. K. Das, J. A. Cooper, and M. R. Melloch, "Metal–oxide–semiconductor capacitors formed by oxidation of polycrystalline silicon on SiC," *Appl. Phys. Lett.*, vol. 70, no. 17, p. 2280, Jun. 1997, doi: 10.1063/1.119262.

[34] K. Piskorski and H. M. Przewlocki, "The methods to determine flat-band voltage VFB in semiconductor of a MOS structure," in *Proc. Int. Conv. MIPRO*, Opatija, Croatia, 2010, pp. 37–42, doi: 978-1-4244-7763-0.

[35] H.-S. Kang *et al.*, "Effect of oxygen species on the positive flat-band voltage shift in Al_2O_3/GaN metal–insulator–semiconductor capacitors with post-deposition annealing," *J. Phys. D, Appl. Phys.*, vol. 46, no. 15, pp. 363–367, 2013.

YANNI ZHANG received the B.S. degree from Xidian University, Xi'an, China, in 2017, where she is currently pursuing the Ph.D. degree with the School of Microelectronics. Her research interest is wide bandgap semiconductor GaN and AlN-based devices.

JINCHENG ZHANG (Member, IEEE) received the M.S. and Ph.D. degrees from Xidian University, Xi'an, China, in 2001 and 2004, respectively, where he is currently a Professor. He has authored and coauthored more than 200 journal and conference papers. His current interests include wide bandgap semiconductor GaN and diamond materials and devices.

ZHUANGZHUANG HU received the B.Eng. degree from Nanchang University, Nanchang, China. He is currently pursuing the Ph.D. degree with the School of Microelectronics, Xidian University, Xi'an.

ZHAOQING FENG received the B.Eng. degree from Xidian University, Xi'an, China, where he is currently pursuing the Ph.D. degree with the School of Microelectronics.

HEPENG ZHANG received the B.S. degree from Xidian University, Xi'an, China, in 2017, where he is currently pursuing the Ph.D. degree with the School of Microelectronics. He mainly engages in the research of AlN/GaN superlattice materials and optimization of RTD devices. Having rich experience in the use of MBE equipment and RTD device fabrication process skills.

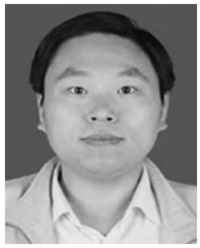

SHENGRUI XU received the B.S. and Ph.D. degrees from Xidian University, Xi'an, China, in 2005 and 2010, respectively.

He is currently a Professor with the School of Microelectronics, Xidian University. His current research interests include GaN-based optoelectronic devices and wide gap-band materials and devices.

ZHIHONG LIU (Senior Member, IEEE) received the B.Sc. degree from Nankai University, China, in 2001, the M.Eng. degree from the Institute of Semiconductors, Chinese Academy of Sciences, China, in 2004, and the Ph.D. degree from Nanyang Technological University (NTU), Singapore, in 2011.

From 2007 to 2011, he was a Research Associate with the Temasek Laboratories, NTU. In 2011, he joined the Singapore-MIT Alliance for Research and Technology Center, as a Postdoctoral Associate, and was promoted to a Research Scientist, in 2014, and a Principal Research Scientist, in 2016. In 2019, he joined Xidian University, China, as a Professor. His current research interests include GaN and other wide bandgap semiconductors based microwave, mmWave, THz devices and MMICs, and also power electronic devices and circuits.

HONG ZHOU (Member, IEEE) received the Ph.D. degree from Purdue University in May 2017.

From June 2017 to February 2018, he was a Postdoctoral Researcher with the University of California at Berkeley. He is currently a Professor with the School of Microelectronics, Xidian University. He has authored and coauthored more than 60 journal and conference papers. His research focuses on fabrication, electrical and thermal measurement, and modeling of negative-capacitance Si FETs, wide bandgap GaN and ultra-wide bandgap ß-Ga_2O_3 based FETs for both DC and RF applications.

YUE HAO (Senior Member, IEEE) is currently a Professor of microelectronics and solid state electronics with Xidian University, Xi'an, China. He has authored and coauthored more than 300 journal and conference papers. His current interests include wide bandgap materials and devices, advanced CMOS devices and technology, semiconductor device reliability physics and failure mechanism, and organic electronics. He is a member of the Chinese Academy of Sciences, China.